Filleting and Rounding
using
Trimmed Tensor Product Surfaces [12]

Gershon Elber[3]

Department of Computer Science

Technion, Israel Institute of Technology

Haifa 32000, Israel

Elaine Cohen

Department of Computer Science

University of Utah

Salt Lake City, UT 84112 USA

Abstract

The tensor product Bézier and NURBs surface representation is frequently exploited in computer aided geometric design. Yet, this representation is inherently rectangular, a topology that does not easily enable the skinning, filleting, and rounding of triangular regions or domains with arbitrary n-sided boundaries.

Modern solid modeling systems support tensor product Bézier and NURBs surfaces with the additional ability to represent the *trimmed* form of these surfaces. This paper explores and presents an approach that allows one to construct regular, nondegenerate positional or tangent plane continuous triangular or n-sided patches, each one as a trimmed tensor product surface. The proposed method is demonstrated on rounding of triangular corners using positional and tangent plane continuity conditions as well as an example of a C^0 hexagonal filleting patch.

---

1 Introduction

Bézier and NURBs surfaces are two common representations that can be frequently found in modern solid modeling systems. The simplicity involved in extending the univariate representation into a bivariate one, as a tensor product, made this topologically rectangular representation a method of choice. Trimmed tensor product surfaces [2, 12] are commonly used to alleviate the deficiency of the tensor product scheme to represent holes in the rectangular patch. Rounding and filleting, a common modeling operation in surface design, is a difficult task using tensor product surfaces. Even for simple objects, topologically triangular representations are necessary for the rounding of corners (see Figure 1). A triangular patch may be represented using three tensor product surfaces and, in general, an n-sided patch can be formed by using n tensor product surfaces. Also, representations of triangular patches [6], S-patches [11] and multivariate splines [14] have been developed but are not as common, possibly because of the computational complexity involved, or lack of crucial algorithms such as subdivision.

One can allow one of the four boundaries of the tensor product surface to degenerate into a point, emulating a triangular patch, as is done in Figure 2. An obvious disadvantage of this approach lays in the fact that one of the partial derivatives vanishes along the degenerated boundary. As a non regular parameterization, the normal of the surface at the degenerated corner cannot be computed as a cross product of partial derivatives. Needless to say, approximating the patch into "fair" polygons becomes a difficult task.

In this paper, an approach is presented in which a single trimmed rectangular regular tensor product surface is used to create patches with a topology of an arbitrary boundary, for which Figure 1 is an example. Positional and plane continuity constraints are considered. This paper is organized as follows. In Section 2, we provide the necessary background.
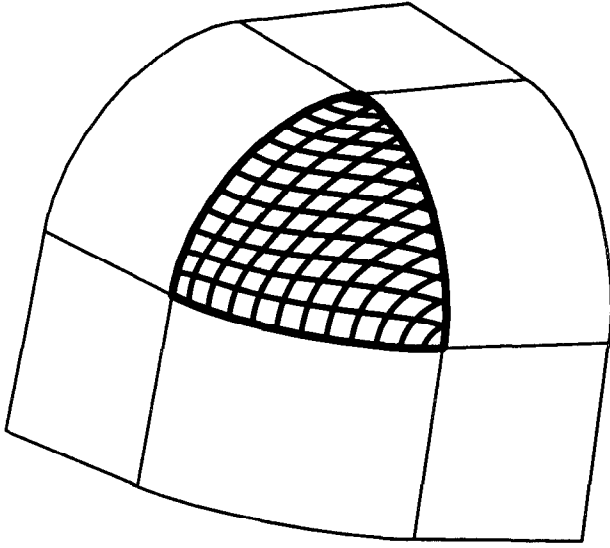
Figure 1: The rounding patch of the corner is topologically a triangle and is represented herein as a trimmed tensor product surface.

Figure 2: A triangular patch constructed with the aid of a degenerated tensor product surface.

Section 3 discusses the constraints for the interpolation of the boundary while Section 4 discusses tangent plane continuity constraints. In Section 5, several examples for triangular filleting are presented. Finally, Section 6 considers the n-sided fillet case and also provides one example of a hexagonal fillet surface. All examples in the paper were created using the Alpha_1 [1] solid modeller, a NURBs based solid modeling system that is developed at the University of Utah.

2 Background

Let $S(u, v)$ be a tensor product Bézier surface,

$$S(u, v) = \sum_{i=0}^{m_u} \sum_{j=0}^{m_v} P_{i,j} B_i^{m_u}(u) B_j^{m_v}(v), \qquad (1)$$

where m_u and m_v are the degrees of the surface.

The partial derivative of $S(u, v)$ with respect to u is equal to,

$$\frac{\partial S(u, v)}{\partial u}$$
$$= \sum_{i=0}^{m_u-1} \sum_{j=0}^{m_v} m_u(P_{i+1,j} - P_{i,j}) B_i^{m_u-1}(u) B_j^{m_v}(v), \qquad (2)$$

and similarly for $\frac{\partial S(u,v)}{\partial v}$ [6].

Given a tensor product Bézier surface (Equation (1)), $S(u, v)$, a degree raised Bézier surface in u is [6],

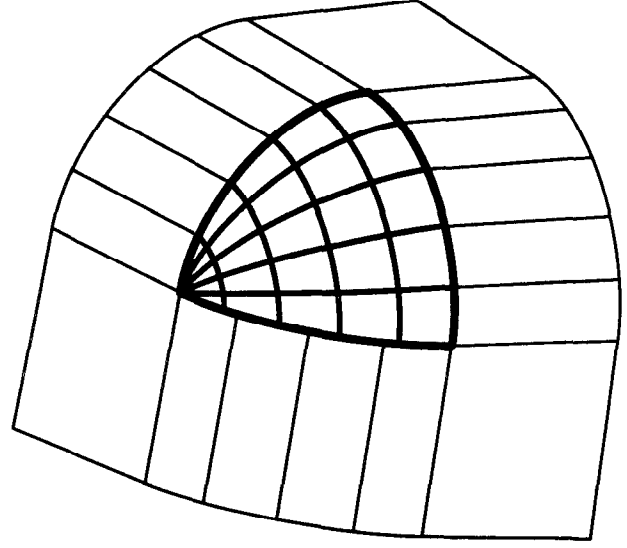$$S(u, v) = \sum_{i=0}^{m_u+1} \sum_{j=0}^{m_v} Q_{i,j} B_i^{m_u+1}(u) B_j^{m_v}(v), \qquad (3)$$

where $Q_{i,j} = \frac{iP_{i-1,j}+(m_u+1-i)P_{i,j}}{m_u+1}$ and the convention that $P_{-1,j} = P_{m_u+1,j} = 0$ [6] is used.

Hence, one can degree raise Equation (2) to be,

$$\frac{\partial S(u, v)}{\partial u}$$
$$= \sum_{i=0}^{m_u-1} \sum_{j=0}^{m_v} m_u(P_{i+1,j} - P_{i,j}) B_i^{m_u-1}(u) B_j^{m_v}(v)$$
$$= \sum_{i=0}^{m_u} \sum_{j=0}^{m_v} ((m_u - i)P_{i+1,j} + (2i - m_u)P_{i,j}$$
$$-iP_{i-1,j}) B_i^{m_u}(u) B_j^{m_v}(v). \qquad (4)$$

Lemma 1 *Let $S(u, v)$ be a polynomial surface in both u and v. If $u = f(t)$, $v = g(t)$ are polynomials in t then the curve $S(f(t), g(t))$ is also a polynomial in t.*

Proof: $S(u, v)$ is a polynomial in both u and v. $f(t), g(t)$ are polynomials in t. A composition $h \circ g$ of two polynomial is also a polynomial. Therefore, $S(f(t), g(t))$ is a univariate polynomial in t. ∎

In [5], a symbolic approach to the computation of this composition for polynomial Bézier curves and surfaces is discussed. In [10], this approach is extended to piecewise polynomial NURBs curves and surfaces. As a direct corollary of Lemma 1, a polynomial curve sketched in the parametric domain of surface S, can be realized as polynomial curve in the Euclidean space as a curve on surface S. Lemma 1 can clearly be extended to (piecewise) rational representations [5].

In this paper and for triangular surface domains defined using polynomial Bézier tensor product surfaces, we will

concentrate on the case of the three lines in the parametric domain of the surface of a surface boundary C_0 of $u = 0$, a surface boundary C_1 of $v = 1$, and the diagonal C_2 of $u = v = t$. Examine $C_2(t) = S(t,t)$, a curve on the Bézier surface S along the diagonal of the parametric domain (see $C_2(t)$ in Figure 3). For $u = v = t$,

$$
\begin{aligned}
C_2(t) &= S(t,t) \\
&= \sum_{i=0}^{m_u} \sum_{j=0}^{m_v} P_{i,j} B_i^{m_u}(t) B_j^{m_v}(t) \\
&= \sum_{k=0}^{m_u+m_v} R_k B_k^{m_u+m_v}(t), \quad\quad (5)
\end{aligned}
$$

with R_k being independent of t because

$$
B_i^{m_u}(t) B_j^{m_v}(t) = \frac{\binom{i}{m_u}\binom{j}{m_v}}{\binom{i+j}{m_u+m_v}} B_{i+j}^{m_u+m_v}(t).
$$

Therefore, $C_2(t)$ is a polynomial curve of degree $m_u + m_v$. See [5] for compositions of varieties with degrees higher than linear and treatment of the (piecewise) rational cases.

3 Positional continuity

Given three polynomial curves, $C_i(t)$, $i = 0...2$, in arbitrary position sharing their end points so they topologically form a triangle, we seek a single tensor product Bézier patch that interpolates all three curves (see Figure 3).

Without loss of generality, we will assume that the sought patch is to interpolate curve $C_0(t)$ along the boundary of $S(0,v)$, to interpolate curve $C_1(t)$ along the boundary of $S(u,1)$, and to interpolate curve $C_2(t)$ along the diagonal of $S(u,u)$. The boundary of $S(0,v)$ is a polynomial in v of degree m_v and the boundary of $S(u,1)$ is a polynomial in u of degree m_u. Furthermore, the diagonal $S(u,u)$ is a polynomial of degree $m_u + m_v$, by Lemma 1 and Equation (5).

Given $k + 1$ independent constraints, and using the fundamental theorem of the algebra, there exists exactly one polynomial of degree k that satisfies these constraints. In the ensuing discussion, we count the degrees of freedom as well as the constraints for each individual coefficient of each vector valued constraint. Therefore, a point in three-space prescribes three constraints, one for each of x, y, and z. One can convert the interpolation problem of the three boundary curves into a set of $3(m_v + 1)$ linear constraints for curve $C_0(t)$, $3(m_u + 1)$ linear constraints for curve $C_1(t)$, and $3(m_u + m_v + 1)$ linear constraints for curve $C_2(t)$. Since the three vertices at the corners are shared by two curves each, $3 * 3$ constraints are redundant and a total of $6(m_u + m_v)$ positional linear constraints are necessary to reproduce $C_i(t)$, $i = 0...2$.

The polynomial patch has $3(m_u + 1)(m_v + 1)$ degrees of freedom, the coefficients of its control points. For example, if $m_u = m_v = m$, in order for a solution to exist, the following must hold,

$$
3(m+1)^2 = 3(m_u+1)(m_v+1) \geq 6(m_u+m_v) = 12m. \quad (6)
$$

For bilinear patches ($m_u = m_v = 1$) the condition becomes an equality. For bi-quadratic and higher degree surfaces, the strict inequality holds, so there are some unconstrained degrees of freedom. Consistency constraints also exist for the three curves of $C_0(t)$, $C_1(t)$, and $C_2(t)$. The degrees of these three curves must be less than or equal to m_v, m_u, and $m_u + m_v$, respectively. These constraints are trivial to satisfy, and we will assume their implicit satisfaction, hereafter. An interesting question is also raised about the way one can exploit the extra degree of freedom, or control points that are not fully prescribed, a question we will partially address in Sections 4 and 5.

The simplest non trivial case is a bi-quadratic (degree 2) surface. The boundaries of $S(0,v)$ and $S(u,1)$ are quadratic polynomial curves while the diagonal is a quartic curve. Because $m_u = m_v = 2$ we have $3(2+1)^2 = 27$ degrees of freedom and only $6(2+2) = 24$ constraints. Any set of independent parametric locations can be selected to form the $k+1$ linear constraints, effectively coercing the interpolation of a degree k curve. Nevertheless, in this work we employ the node points or the Greville Abscissae [7], points that are typically more stable, numerically. In Figure 4, a bi-quadratic surface is coerced to interpolate the eight points q_i, $i = 0...7$ yielding 24 constraints, while exploiting its 27 degrees of freedom from the nine control points p_{jk}, $j,k = 0...2$. As a result, this biquadratic tensor product surface interpolates the three given curves.

4 Tangent Plane Continuity

Given three polynomial curves, $C_i(t)$, $i = 0...2$, in arbitrary position sharing their end points, so they topologically form a triangle, and three polynomial vector field curves, $D_i(t)$, $i = 0...2$, we seek a Bézier patch, S, that interpolates all three $C_i(t)$ curves so that the tangent plane of S at $C_i(t)$ contains $D_i(t)$ (see Figure 5). We further assume that $D_i(t)$ and $\frac{C_i(t)}{dt}$ are independent, that is, $D_i(t) \neq \alpha \frac{C_i(t)}{dt}$, $\forall t$.

Without loss of generality, we will assume that the sought patch is to interpolate curve C_0 (D_0) along $S(0,v)$ boundary, to interpolate curve C_1 (D_1) along $S(u,1)$ boundary, and to interpolate curve C_2 (D_2) along the diagonal of $S(u,u)$.

The vector field curves, $D_i(t)$, can be prescribed by the three neighboring patches of the triangular patch S. Then, the $D_i(t)$ are derived as the cross boundary derivatives of these three neighboring patches. Alternatively, the $D_i(t)$ can be implicitly specified as a difference of two Euclidean curves, as in Figure 5.

In Section 2, a representation to the partial derivatives of the surface is constructed, that exploits the *same basis functions* as the original surface. The partial derivatives are elevated to the same degree using degree raising. By elevating the differentiated surface to the same degrees as the original surface, it is straightforward to use the same basis functions for representing both the positional and tangent plane continuity constraints. Fewer evaluations of basis functions are therefore necessary in the construction of the
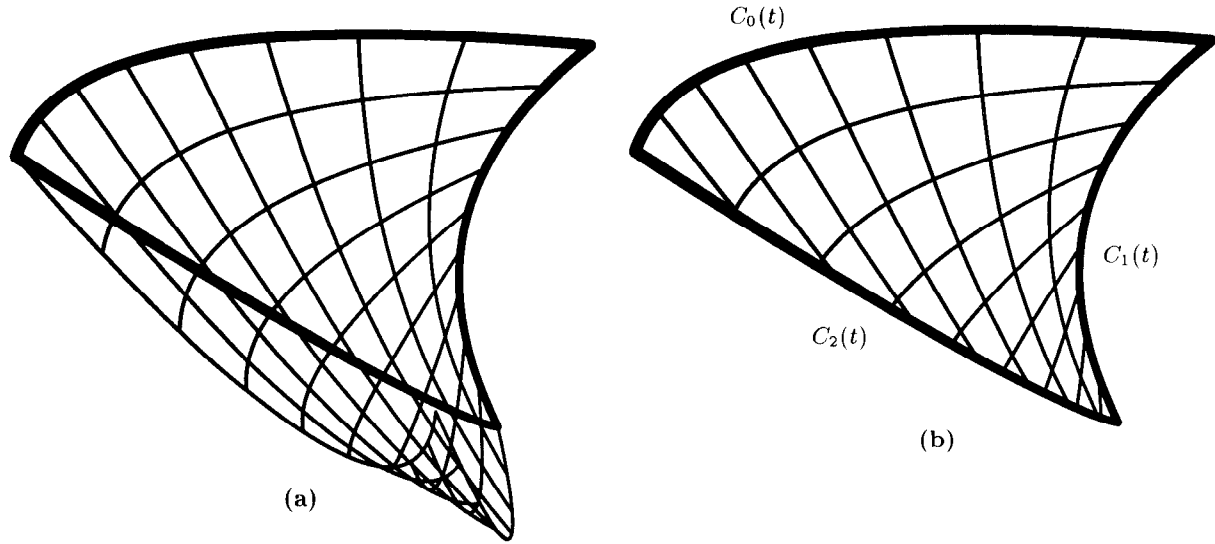
Figure 3: A Bézier patch interpolating curve $C_0(t)$ along $S(0, v)$ boundary, curve $C_1(t)$ along $S(u, 1)$ boundary, and curve $C_2(t)$ along $S(u, u)$ diagonal. In (a), the full surface is shown while in (b) only the non-trimmed triangular domain is displayed.
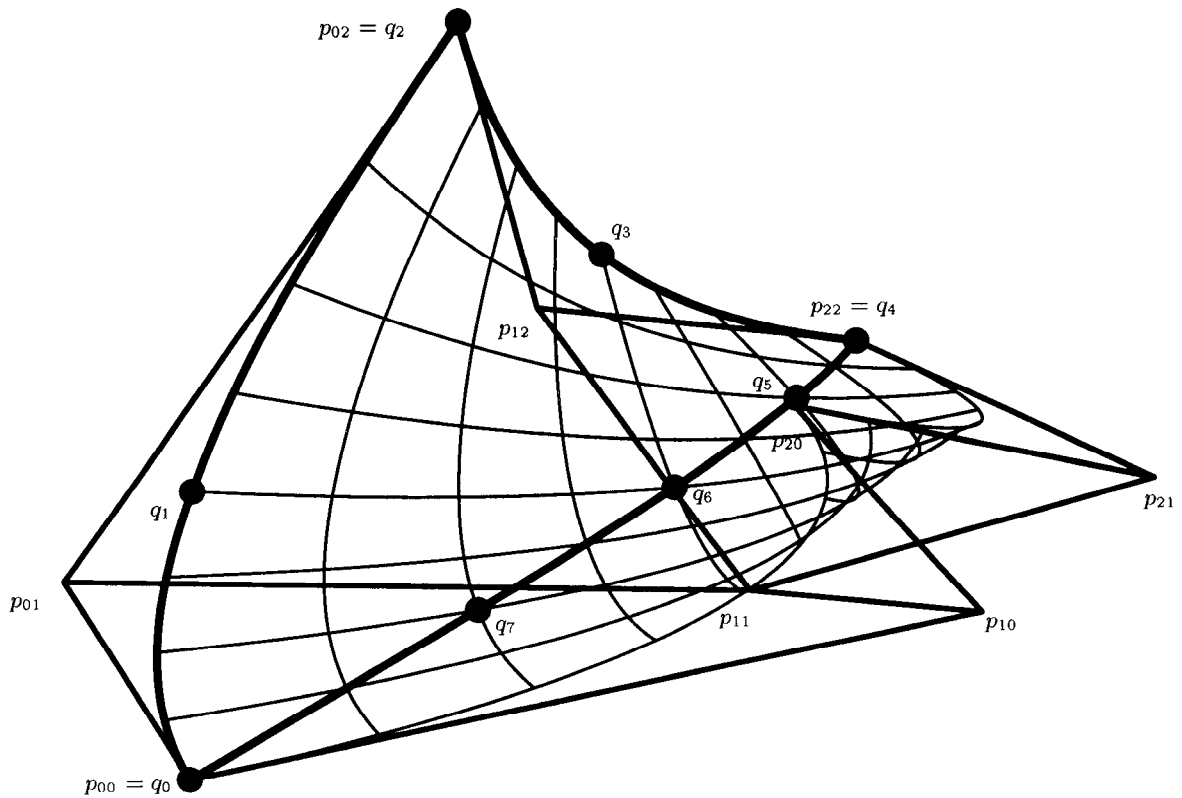

Figure 4: This bi-quadratic Bézier patch is coerced to interpolate the three space curves (thick lines) by solving an under-constrained linear system with 24 linear constraint equations and 27 unknown or degrees of freedom.
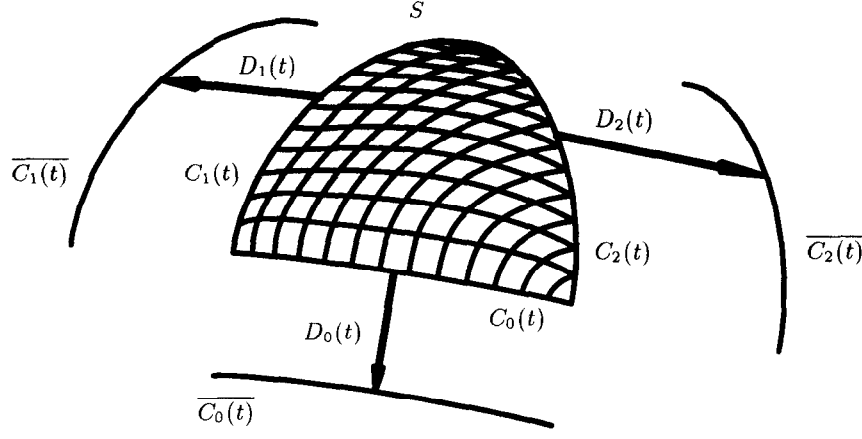
209

Figure 5: A Bézier patch S interpolates curve $C_0(t)$ along $S(0, v)$ boundary, curve $C_1(t)$ along $S(u, 1)$ boundary, and curve $C_2(t)$ along the diagonal of $S(u, u)$. Furthermore, the tangent plane of S at $C_i(t)$ contains $D_i(t)$.

constraints as a linear system for the purpose of resolving the tangent plane continuity.

Setting $u = 0$ in Equation (4), leads to a simplified expression for $\frac{\partial S}{\partial u}$. Because $B_i^{m_u}(0) = \delta_{i,0}$, where δ denotes the Kronecker delta,

$$
\left. \frac{\partial S(u, v)}{\partial u} \right|_{u=0}
$$
$$
= \sum_{i=0}^{m_u} \sum_{j=0}^{m_v} ((m_u - i)P_{i+1,j} + (2i - m_u)P_{i,j}
$$
$$
- iP_{i-1,j}) B_i^{m_u}(u) B_j^{m_v}(v)
$$
$$
= m_u \sum_{j=0}^{m_v} (P_{1,j} - P_{0,j}) B_j^{m_v}(v). \tag{7}
$$

Similarly, for $v = 1$, $B_j^{m_v}(1) = \delta_{j,m_v}$ and $\frac{\partial S(u,v)}{\partial v}$ simplifies to,

$$
\left. \frac{\partial S(u, v)}{\partial v} \right|_{v=1} = m_v \sum_{i=0}^{m_u} (P_{i,m_v} - P_{i,m_v-1}) B_i^{m_u}(u). \tag{8}
$$

The partial derivatives along the diagonal are affected by the entire set of control points, since none of the Bézier basis functions is zero for interior points. Using Equation (4),

$$
\frac{\partial S(v, v)}{\partial u}
$$
$$
= \sum_{i=0}^{m_u} \sum_{j=0}^{m_v} ((m_u - i)P_{i+1,j} + (2i - m_u)P_{i,j} -
$$
$$
iP_{i-1,j}) B_i^{m_u}(v) B_j^{m_v}(v). \tag{9}
$$

Since the tangent plane constraints, $D_i(t)$, are represented as vector field polynomials, it is possible to coerce the interpolated triangular patch to satisfy the tangent plane constraints using only linear systems of equations.

The formulated problem is overconstrained since the tangent planes are already fully prescribed at the three corners

of the triangular patch by the positional constraints. In the ensuing discussion, it is therefore assumed that the $D_i(t)$'s are coplanar with the planes prescribed by the positional constraints, at the corners.

A simple approach to formulating the tangent plane continuity constraints is to add linear constraints that will force the interpolated patch to have its cross partial at $C_i(t)$ match that of $D_i(t)$. However, since only tangent plane continuity is necessary, the C^1 parametric continuity constraints may be relaxed into G^1 geometric continuity constraints. In [4], the necessary and sufficient conditions for tangent plane continuity are derived for Bézier surfaces. Consider the derivative along the mutual boundary of the two patches as well as the two cross boundary derivatives of the two patches along that boundary. Then, [4] defines the tangent plane continuity conditions in terms of the coplanarity of there three derivative vector fields. The G^1 geometric continuity continuity constraints can also be formulated as linear constraints, as we do herein. The (unnormalized) surface normal at $C_i(t)$ is fully specified by $C_i(t)$ and $D_i(t)$ and is equal to

$$
N_i(t) = D_i(t) \times \frac{dC_i(t)}{dt}. \tag{10}
$$

Extending [3, 8, 9], we define a linear constraint for a surface cross derivative along an entire boundary. For example, along the surface boundary curve $S(0, v)$, $\frac{\partial S(u,v)}{\partial u}$ must be perpendicular to $N_i(v)$,

$$
0 = \left\langle N_i(v), \left(\left. \frac{\partial S(u, v)}{\partial u} \right|_{u=0} \right) \right\rangle. \tag{11}
$$

The constraint in Equation (11) is linear in the control points of the patch. In [3, 8, 9], such constraints are used to enforce normal direction interpolation at a discrete set of locations, while each normal direction interpolation is expressed as a pair of linear constraints on the two partial derivatives of the surface. Because both $\frac{\partial S(u,v)}{\partial u}$ and $N_i(v)$
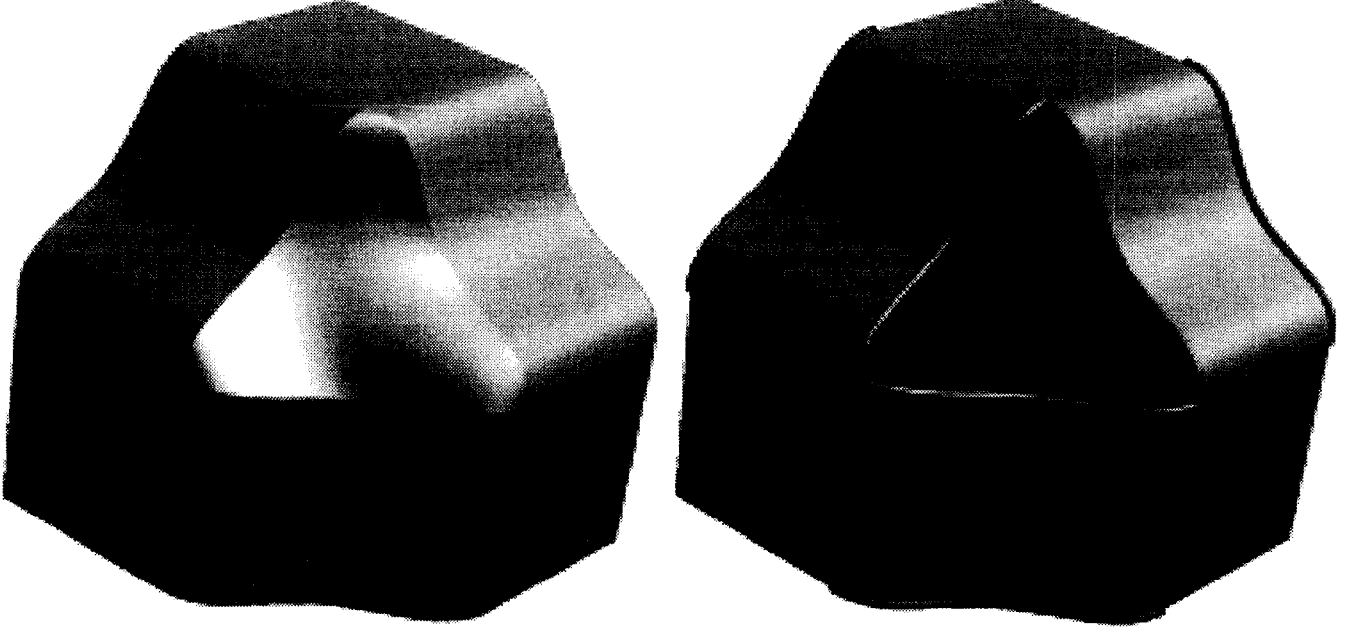
210

Figure 6: Positional continuity for a triangular trimmed tensor product surface. Compare with Figure 7. Both images in this figure are identical while the right one also presents the $C_i(t)$ curves as well as the curves used to derive $D_i(t)$.

(Equation (10)) are polynomials, their inner product (Equation (11)) is also a polynomial. Further, this polynomial must the zero polynomial, a constraint that can be satisfied if and only if all the coefficients of all its basis functions are identically zero.

Assume the neighboring surfaces are all degree n_u by n_v, and that the triangular patch we attempt to construct is degree m_u by m_v. For simplicity we also assume that $n_u = n_v = n$ and $m_u = m_v = m$. Hence, $C_i(t)$ and $D_i(t)$ are degree n curves. Further, $N_i(t)$ (Equation (10)) is degree $n + (n-1)$, and the constant zero polynomial of Equation (11) is degree $n+(n-1)+m$ for the two boundaries of the triangular patch that are also boundaries of the tensor product surface, and is degree $n+(n-1)+(2m-1)$ for the third boundary of the triangular patch, which is a diagonal the tensor product surfaces. Using the fundamental theorem of the algebra, $n+(n-1)+m+1$ linear constraints at different v parameter values of Equation (11) are sufficient to coerce Equation (11) to be identically zero at the boundary of the patch and $n + (n-1)+(2m-1)+1$ linear constraints are sufficient for the diagonal.

We are now ready to count the number of constraints that are needed for tangent plane continuity. For the positional constraints, each point contributes three constraint. In contrast, for the plane continuity constraints, we introduce scalar valued equations. Each set of tangent plane continuity constraints of a boundary has two of its degrees of freedom already specified, at the three corners of the triangular patch, by the positional constraints. Accumulating the tangent plane continuity constraints of all three bound-

aries,

$$(n + (n-1) + m + 1) * 2$$
$$+ (n + (n-1) + (2m-1) + 1) - 2 * 3$$
$$= 6n + 4m - 7. \tag{12}$$

Combined with the necessary (vector valued) positional constraints (Equation (6)), the number of constraints should be not greater than the number of degrees of freedom, $3(m + 1)^2$,

$$3(m+1)^2 \geq 6n + 4m - 7 + 12m$$
$$= 6n + 16m - 7, \tag{13}$$

or,

$$3m^2 - 10m - 6n + 10 \geq 0. \tag{14}$$

The minimal degree m that satisfies inequality (14) is therefore the ceiling (minimal upper integer bound) of the larger zero of quadratic inequality (14),

$$m = ceil\left(\frac{10 + \sqrt{100 - 12(10 - 6n)}}{6}\right). \tag{15}$$

For example for both $n = 2$ (bi-quadratic neighboring patch) with $m = 4$ (quartic trimmed tensor product fillet patch), and $n = 3$ (bi-cubic neighboring patch) with $m = 4$ (quartic trimmed tensor product fillet patch) satisfy that relationship constraint.

One can exploit either $\frac{\partial S}{\partial u}$, $\frac{\partial S}{\partial v}$, or any linear combination of the two partial derivatives to yield an equivalent system
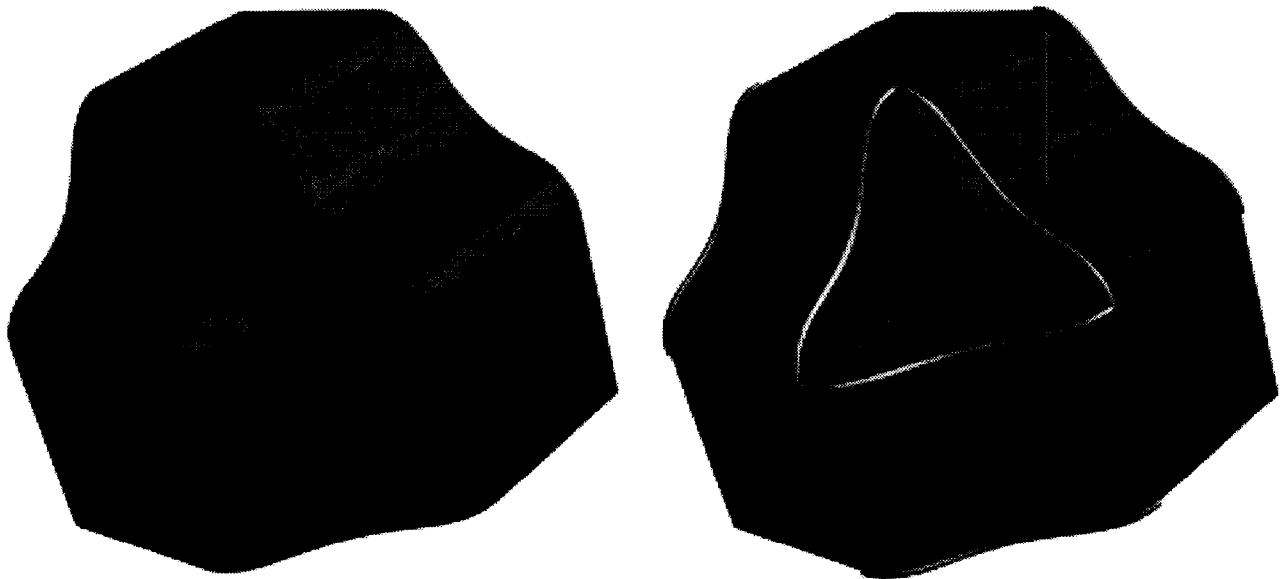
Figure 7: Tangent plane continuity for a triangular trimmed tensor product surface. Compare with Figure 6. The three $C_i(t)$ curves as well as the three $D_i(t)$ vector fields are of degree four and the trimmed triangular patch is bi-quartic (degree five by degree five). Both images in this figures are identical while the right one also presents the $C_i(t)$ curves along with the curves used to derive $D_i(t)$.

of linear constraints for the tangent plane continuity along the diagonal of the patch, provided that $\frac{\partial S}{\partial u}$, $\frac{\partial S}{\partial v}$, and $\frac{dC_3(t)}{dt}$ are nowhere collinear in the domain. This, due to the fact that $\frac{\partial S}{\partial u}$, $\frac{\partial S}{\partial v}$, and $\frac{dC_3(t)}{dt}$ are all coplanar.

5 Examples

Rounding and filleting of corners is an obvious example that might benefit from the proposed method. Figure 6 shows a trimmed Bézier surface interpolating the three corner curves providing only positional continuity. Figure 7 shows the same patch, this time with tangent plane continuity. Figures 8 and 9 show same additional triangular patch interpolated using the proposed scheme. In all the figures, the $D_i(t)$'s were specified as vector field curves.

The interpolation problem resulting from the constraint satisfaction is usually under-constrained. In other words, Equations (6) or (14) are strict inequalities. One can use the degrees of freedom that are left to coerce the patch to interpolate additional *interior* points and/or tangents and normals as is done, for example, in [15], or to satisfy some global smoothness criteria. Figure 10 shows several triangular patches of rounded corners that interpolate additional prescribed interior points.

The interpolated surface may self intersect as can be seen in Figure 11, and *surface fairness* techniques can be considered in the proposed scheme to alleviate this problem, ex-

ploiting the free degrees of freedom. The method suggested in [15] that minimizes stretch (magnitude of first derivatives) and bending (magnitude of second derivatives) over the surface domain, might be combined with the triangular skinning method proposed herein.

Figure 12 is used to raise a point of caution. While the resulting surfaces do interpolate their constraints, the control meshes can assume an unexpected shape due to the interpolatory approach employed. This unpredictable behavior is typically more significant in the unconstraint triangular region of the tensor product surface. This behavior might of importance if, for example, tight bounding boxes for these surfaces are necessary, and the bounding boxes of the control meshes are exploited

6 n-sided Surface Patches

The domain that trims the tensor product surface can be arbitrarily shaped and it is not limited to a triangular shape as in the previous sections. Given a patch, S, of a degree of $m \times m$, every isoparametric curve of S will be of degree m as well. Any straight line in the interior of the parametric space of the surface will be elevated into a curve of degree $2m$ (See Equation (5)). Therefore, one can create an arbitrary n-sided freeform patch by trimming an n-sided freeform domain out of a tensor product surface. At the worst case, all n sides are interior to the tensor product surface and none is
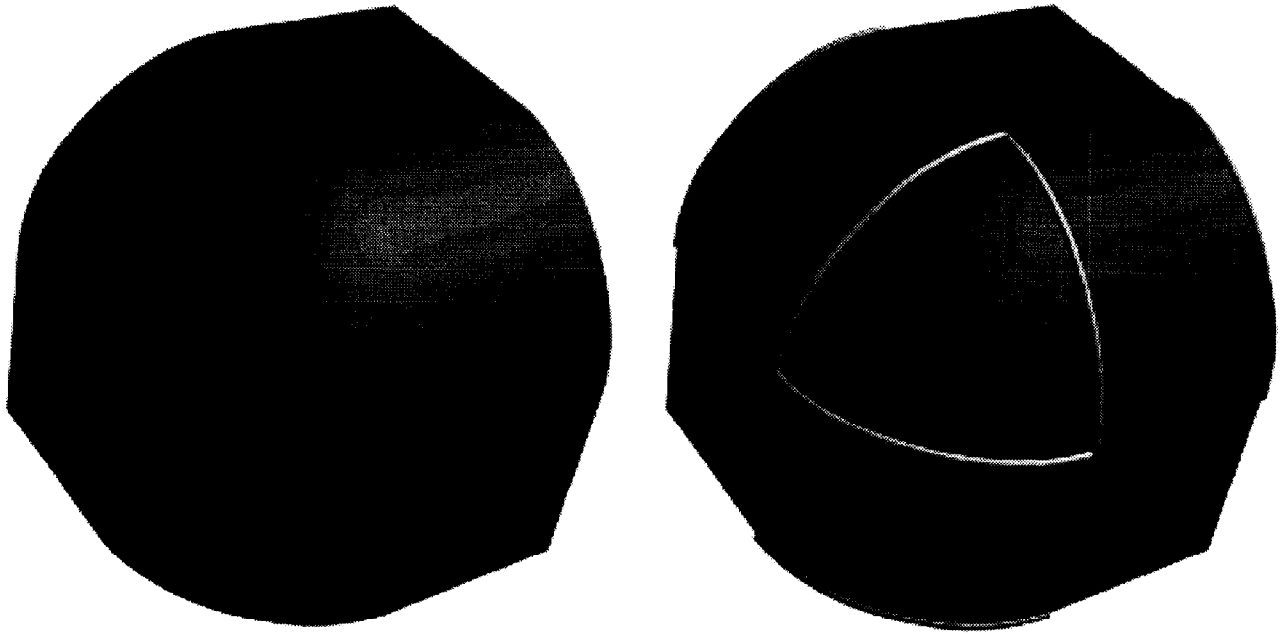
Figure 8: Tangent plane continuity for a triangular trimmed tensor product surface. The three $C_i(t)$ curves as well as the three $D_i(t)$ vector fields are cubic and the trimmed triangular patch is bi-quartic. Both images in this figure are identical while the right one also presents the $C_i(t)$ curves along with the curves used to derive $D_i(t)$.
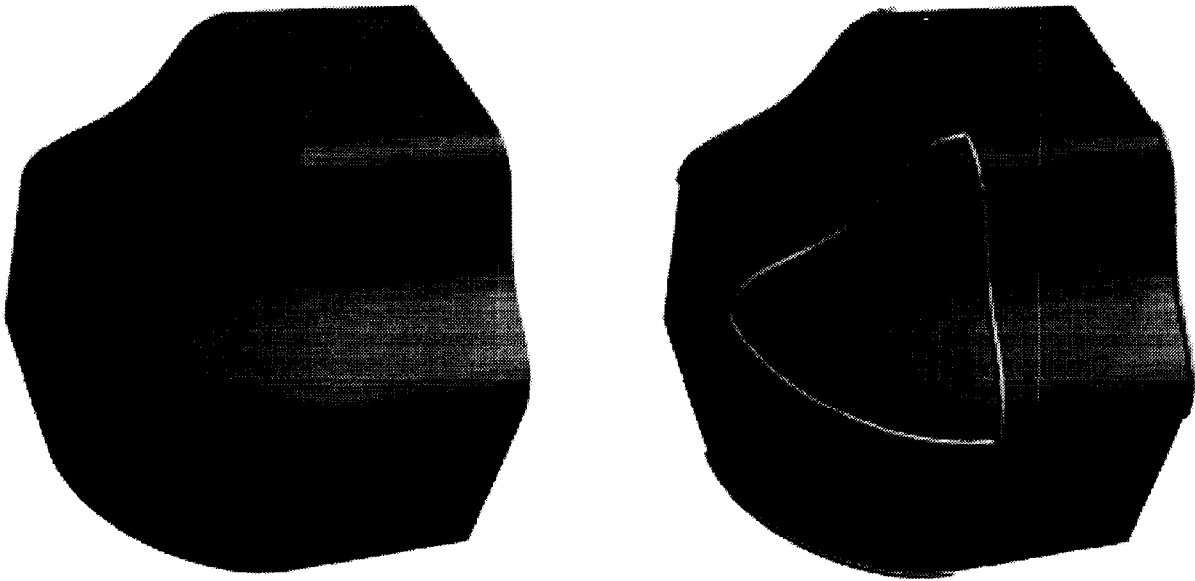

Figure 9: Tangent plane continuity for a triangular trimmed tensor product surface. The three $C_i(t)$ curves as well as the three $D_i(t)$ vector fields are of degrees three, four, and four, and the trimmed triangular patch is bi-quartic. Both images in this figure are identical while the right one also presents the $C_i(t)$ curves along with the curves used to derive $D_i(t)$.
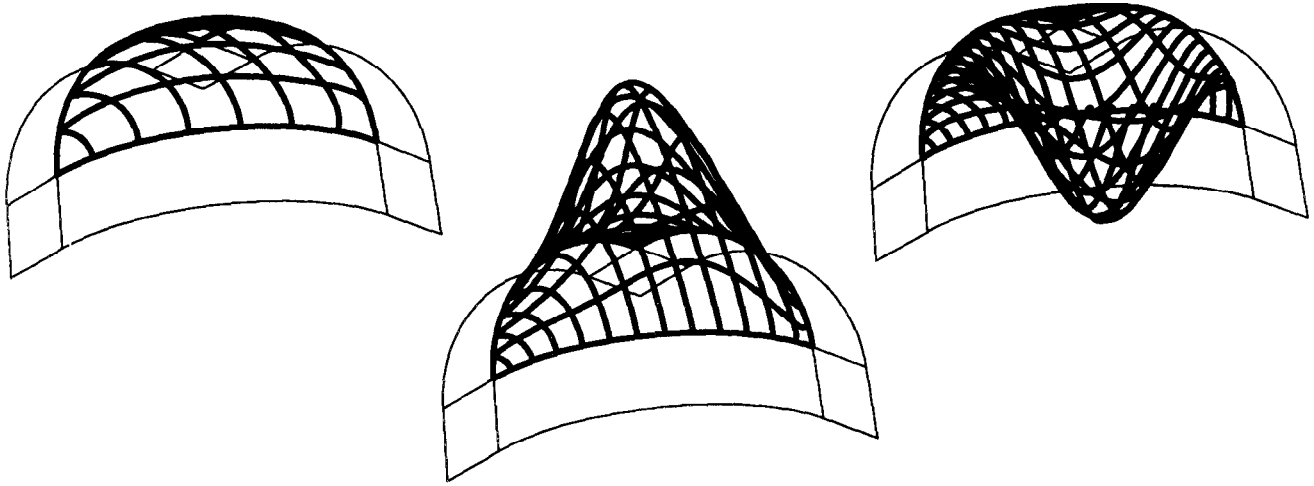
213

Figure 10: Tangent plane continuity with the additional interpolation of interior points at different locations.
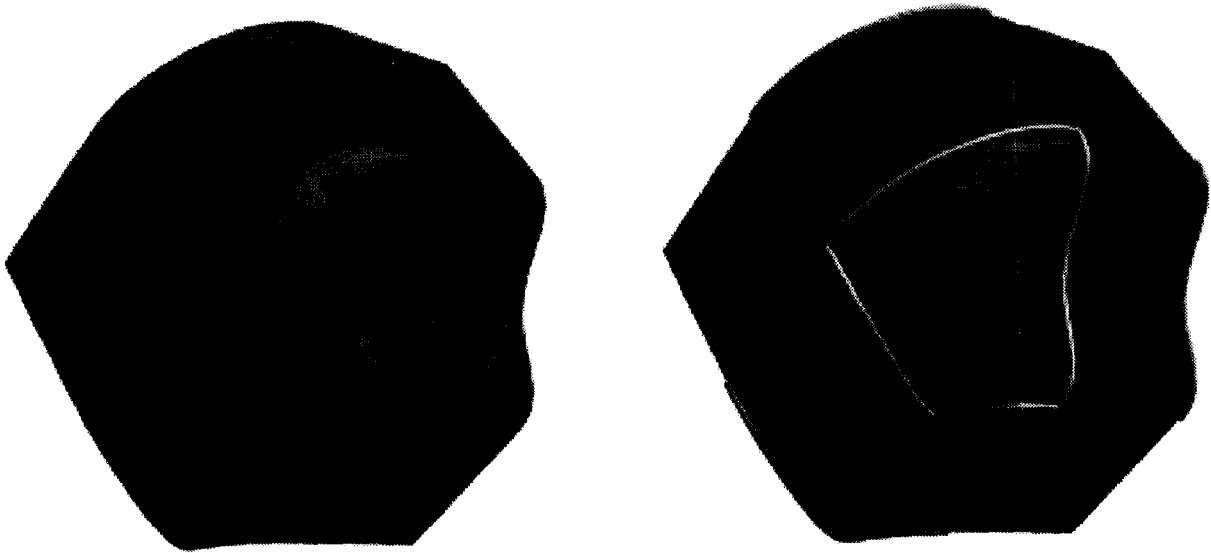

Figure 11: While tangent plane continuous, the interpolated triangular patch can self intersect as is evident in this Figure. Both images in this figure are identical while the right one also presents the $C_i(t)$ curves along with the curves used to derive $D_i(t)$
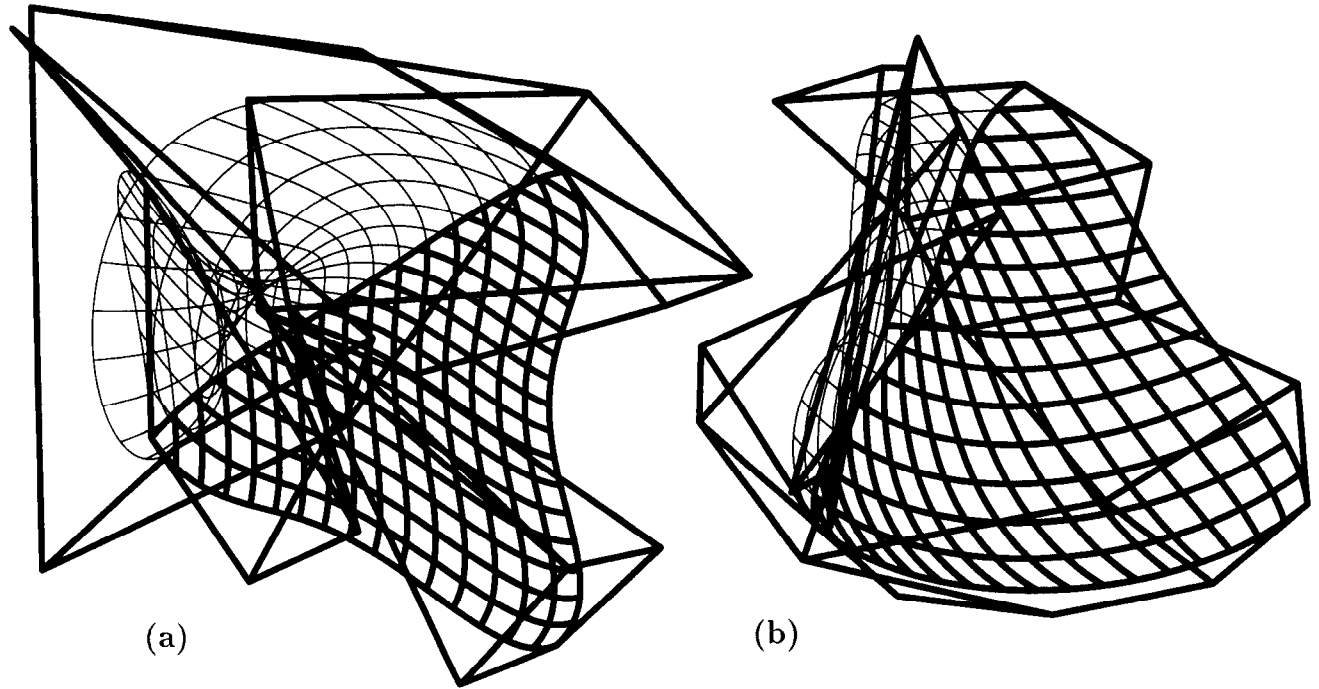
Figure 12: The control mesh of the interpolated triangular meshes can assume unpredictable shapes, especially in the trimmed out domain, as is demonstrated herein for the patches computed in Figures 7 and 9.

in an iso-parametric direction. Hence, $3*(2m+1)*n$ degrees of freedom are necessary, where $3(m+1)^2$ are available, and it is clear that given n, there is always a sufficient m that satisfies the constraint equation of $3(m+1)^2 \geq 3*(2m+1)*n$.

Consider, for example, the case of an hexagonal fillet patch (See Figure 13 (a)). Herein, four boundaries out of the six boundaries of the hexagonal fillet patch are selected to be on (part of) the boundaries of the tensor product surface while two additional boundary curves of the hexagonal fillet are diagonal straight lines in the interior of the parametric domain of the tensor product trimmed surface. Hence, the number of constraint imposed by the four tensor product boundary curves is $4*3(m+1)$ and by the two diagonal boundary curves is $2*3(2m+1)$. Yet, the six vertices of the boundaries of the hexagonal fillet patch are constrained twice. Hence, the total number of positional constraint is $4*3(m+1) + 2*3(2m+1) - 3*6 = 24m$. Because $24m$ must be less than or equal to $3(m+1)^2$, $m \geq 6$ can be employed. Figure 13(b) shows one example of a C^0 continuous hexagonal fillet patch exploiting this proposed scheme, for a six-sided fillet patch at a corner.

7 Conclusion

An approach to represent triangular or n-sided patches using trimmed tensor product rectangular patches was presented. The proposed method is able to represent non degenerated triangular patches by utilizing tools that are available in most modern solid modeling systems, namely tensor prod-

uct polynomial surface representation and trimmed surface support.

We have demonstrated the construction of rounded triangular polynomial corners of various degrees as well as an hexagonal filleting, using the Bézier representation. One can extend the proposed approach to support the NURBs representation since algorithms for the computation and representation of the composition operation [10], derivatives [6], and products [5, 13] of NURBs as NURBs do exists.

Arbitrary polygonal regions can be defined in a parametric domain of a surface by using only linear functions of the form $u = av + b$. Given a tensor product surface $S(u, v)$ of degree m_u by m_v, the boundary curve of the n-sided patch is composed as $S(av + b, v)$ into the interior of the tensor product surface, is of degree $m_u + m_v$ in v, and it can be computed symbolically. Hence, the number of positional and tangent plane continuity constraints grow linearly with the degree while the number of degrees of freedom grow quadratically with the degree. This suggests there always exists a patch with a sufficient degree that is able to satisfy all the necessary constraints.

REFERENCES

[1] Alpha_1. Alpha_1 User's Manual, University of Utah, Computer Science, 1992.

[2] M. S. Casale. Free-form solid modeling with trimmed surface patches. Numeric Computation. IEEE Com-
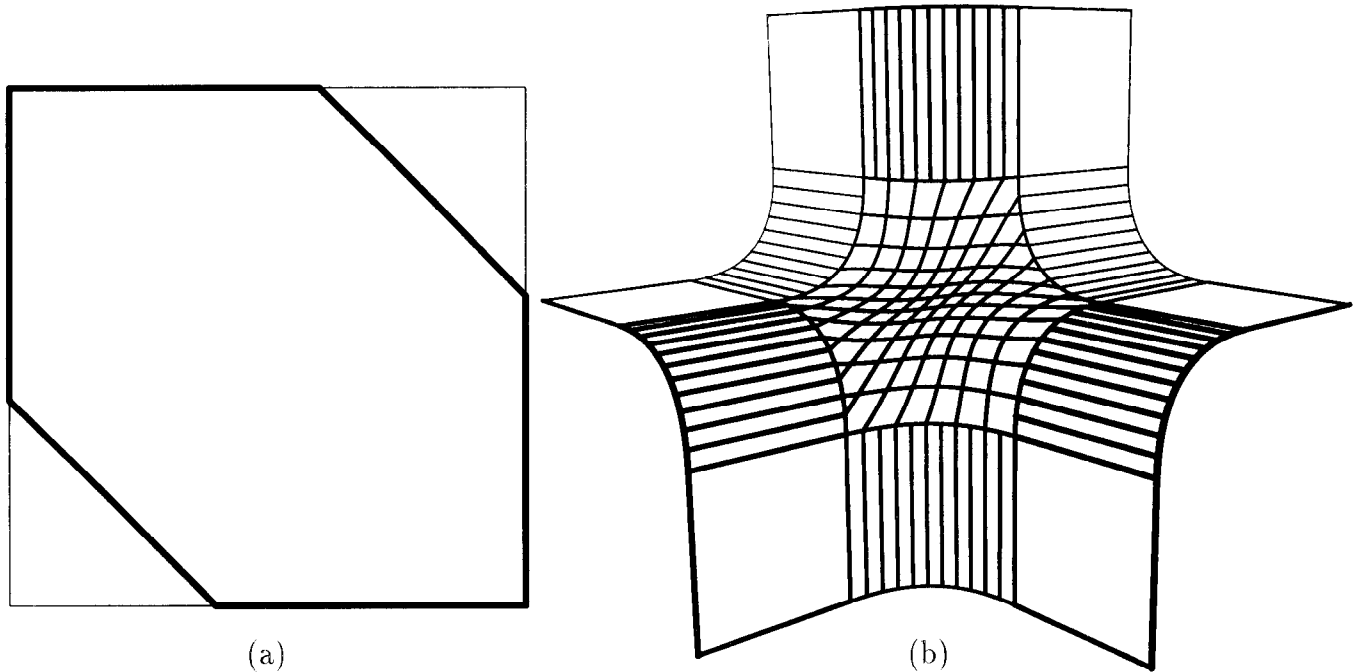
(a)   (b)

Figure 13: A tensor product surface is trimmed twice to form a six sided patch or an hexagonal fillet patch. In (a), the trimmed parametric domain is shown. In (b), the actual Euclidean result is presented.

puter Graphics and Applications, Vol. 7, no. 1, pp 33-43, January 1987.

[3] G. Celniker and W. Welch. Linear Constraints for Deformable B-spline Surfaces. Computer Graphics, Vol 25, No. 2, pp 165-170, March 1992 (1992 Symposium on Interactive 3D Graphics).

[4] T. D. DeRose. Necessary and Sufficient Conditions for Tangent Plane Continuity of Bézier Surfaces. Computer Aided Geometric Design, Vol 7, pp 165-179, 1990.

[5] G. Elber. Free Form Surface Analysis using a Hybrid of Symbolic and Numeric Computation. Ph.D. thesis, University of Utah, Computer Science Department, 1992.

[6] G. Farin. Curves and Surfaces for Computer Aided Geometric Design Academic Press, Inc. Second Edition 1990.

[7] G. Farin. NURB Curves and Surfaces from Projective Geometry to Practical Use. A. K. Peters, Wellesley, Massachusetts, 1994.

[8] B. Fowler. Geometric Manipulation of Tensor Product Surfaces. Computer Graphics, Vol 25, No. 2, pp 101-108, March 1992 (1992 Symposium on Interactive 3D Graphics).

[9] H. Hoppe, T. DeRose, T. Duchamp, J. McDonald, and W.Stuetzle. Mesh Optimization. Computer Graphics, Vol 27, pp 19-26, August 1993 (Siggraph 1993).

[10] K. Kim. Blending Parametric Surfaces. M.S. Thesis, University of Utah, Computer Science Department, August 1992.

[11] C. Loop and Tony DeRose. Generalized B-Spline Surfaces of Arbitrary Topology. Computer Graphics, Vol. 4, no. 4, pp 347-356, August 1990, (Siggraph 1990).

[12] T. McCollough. Support for Trimmed Surfaces. M.S. Thesis, University of Utah, Computer Science Department, 1988.

[13] K. Morken. Some Identities for Products and Degree Raising of Splines. To appear in the Journal of Constructive Approximation.

[14] T. I. Mueller. Geometric Modelling with Multivariate B-Splines. Ph.D. Thesis, University of Utah, Computer Science Department, 1986.

[15] W. Welch and A. Witkin. Variational Surface Modeling. Computer Graphics, Vol 26, No. 2, pp 157-166, July 1992 (Siggraph 1992).

216